NANO LETTERS

Letter

pubs.acs.org/NanoLett

Spectroscopic Determination of Phonon Lifetimes in Rhenium-Doped MoS_2 Nanoparticles

Qi -C. Sun,[§,†] Dipanjan Mazumdar,[†] Lena Yadgarov,[‡] Rita Rosentsveig,[‡] Reshef Tenne,[‡] and Janice L. Musfeldt*[,†]

[†]Department of Chemistry, University of Tennessee, Knoxville, Tennessee 37996, United States

[‡]Department of Materials and Interfaces, Weizmann Institute of Science, Rehovot 76100, Israel

Supporting Information

ABSTRACT: We investigated the infrared vibrational properties of pristine and Re-substituted MoS_2 nanoparticles and analyzed the extracted phonon lifetimes in terms of multiple scattering events. Our measurements reveal both size- and doping-dependent changes that we attribute to grain boundary scattering and charge and mass effects, respectively. By contrast, Born charge is affected only by size. These findings illustrate the utility of reaching beyond traditional bulk semiconductors and quantum dots to explore how doping and confinement impact carrier-phonon interactions in low-dimensional semiconducting nanomaterials.

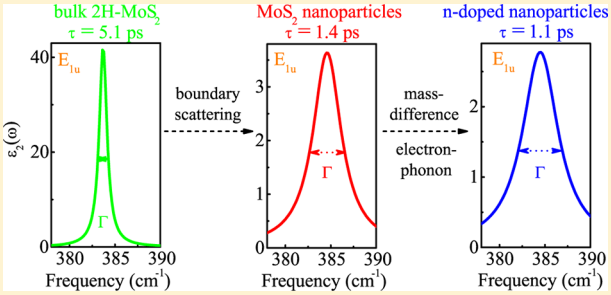

KEYWORDS: *Phonon lifetime, chalcogenides, infrared spectroscopy, layered materials, nanoparticles*

Phonons and their interactions govern the properties of many complex materials including ferroelectrics, thermoelectrics, and multiferroics.[1−3] Key to a number of electronics applications for semiconductors is an understanding of carrier dynamics, and in particular, phonon scattering.[4,5] Vibrational property measurements directly uncover interactions between carriers and optical phonons, and the phonon lifetimes (τ's) thus extracted (Figure 1) are valuable benchmarks for device performance.[3,4,6−10] Traditional, high-quality polar semiconductors like GaAs, ZnSe, and GaN have τ's between 2 and 10 ps.[4,7−9] Phonon lifetimes in a solid are strongly affected by anharmonic interactions as well as scattering from defects and impurities,[6] and as a result they influence everything from carrier mobilities and the dynamical processes of charge carriers[11] to the thermoelectric figure of merit.[3] τ is also important for determining the total energy loss rate, a concept that has been used to assess confinement in microelectronic devices.[10] As the size of semiconductor electronics becomes smaller, carrier-phonon interactions have a greater impact on device performance, and quantitative information on phonon lifetimes becomes even more critical. The situation also becomes more complicated because phonon lifetimes in nanoscale objects are heavily influenced by multiple scattering events.[12,13] MoS_2 attracted our attention as a system with which to reach beyond conventional semiconductors and investigate phonon lifetimes under both finite size and n-doping conditions. It displays a number of different morphologies including various two-dimensional layered structures like hexagonal 2H-MoS_2, nanotubes, nanoparticles (herein abbreviated IF-MoS_2 where IF = inorganic fullerene), and nanosheets.[14−16] The recent discovery of high quality Re-doped nanoparticles (henceforth Re:IF-MoS_2 to denote Re as a substitutional dopant),[17−20] the interesting electronic nature of

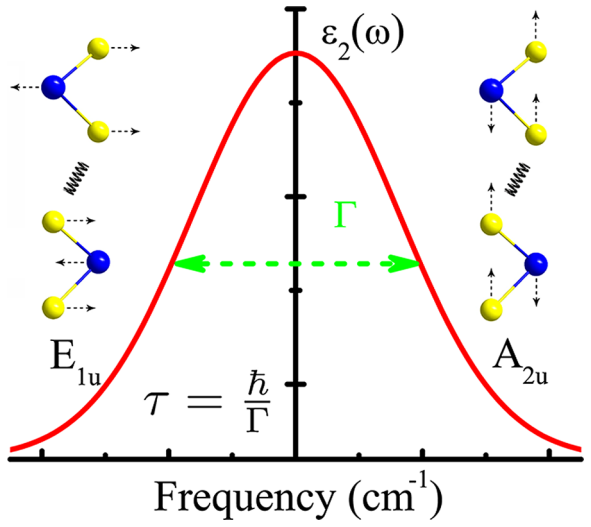

Figure 1. Schematic view of a phonon with typical Lorenzian line shape illustrating how the full width at half-maximum Γ is related to the lifetime τ as $\tau = \hbar/\Gamma$. Clearly phonon linewith and lifetime are expressions of the Heisenberg uncertainty principle.[4,45] Schematic views of the displacement patterns for the infrared-active E_{1u} and A_{2u} vibrational modes in 2H-MoS_2 are also included.[37,38].

Received: March 23, 2013
Revised: April 21, 2013
Published: April 23, 2013

these compounds,[21−27] and their superior lubrication properties[18,20,28−31] motivates our extended analysis. What differentiates our work from prior efforts on semiconductor quantum dots[32,33] is the two-dimensional nature of MoS_2 and the fact that the confined electrons do not have a well-defined periodicity.

In this Letter, we report the discovery of dramatic size- and doping-induced changes in the phonon lifetimes of MoS_2 nanoparticles that we analyze in terms of multiple scattering events. Our spectroscopic measurements reveal that while the lifetime of 2H-MoS_2 is similar in magnitude to that of semiconductors like GaAs, τ of the nanoparticles is 50% smaller. The n-doping reduces the phonon lifetime even further. We discuss these trends in terms of grain boundary scattering and charge and mass effects, respectively. By contrast, an analysis of chemical bonding as determined by Born effective charge, local effective charge, polarizability, and the spring constant, uncovers only size effects. Taken together, these findings advance the understanding of carrier−phonon interactions in low-dimensional semiconducting nanomaterials, extend the quantitative relationship between Re concentration and carrier density[19,27] to include one of the factors that influences mobility and charge dynamics, and highlight the unique character and potential of n-doped chalcogenide nanoparticles for electronics[21,22,24,27] and solid state lubrication[20,28−31] applications.

Re-doped (0.0106 and 0.18%) IF-MoS_2 (Re:IF-MoS_2) and IF-MoS_2 were synthesized in a gas phase reaction from MoO_3 powder by a three-step procedure in a vertical bed reactor.[20,34] The resulting nanoparticles ranged in size from 50 to 140 nm in diameter with a mean size of 80 nm. Formal 0.12 and 0.42% Re concentrations in the ReO_3/MoO_3 starting material yielded actual dopant concentrations of 0.0106 and 0.18% in the nanoparticles.[19] Re engages in substitutional rather than intercalative doping. The structure[35] does not seem to be influenced by doping, although aggregation of ReS_2 islands cannot be excluded, especially at the highest doping level.[19] 2H-MoS_2 was purchased directly from Alfa Aesar (99%). The platelet size was ∼44 μm. Pressed pellets were prepared for investigating the optical properties of these materials. Densities of the compresses were, however, only ∼3.5 g/cm^3 rather than the theoretically expected value of 4.996 g/cm^3 that is realized in a 2H-MoS_2 single crystal. Sample densities were therefore ∼70% of the single crystal density, a difference that we correct for in our analysis.[39] Near normal reflectance was measured over a wide frequency range (25−52 000 cm^{-1}) using a series of spectrometers, and a 2000 Å aluminum overcoat was used to correct for scattering effects. A Lorenzian oscillator fitting analysis was used to extract the observed oscillator parameters.[40] The intrinsic oscillator parameters were obtained from the observed fit parameters by applying density, orientational, and scattering corrections as detailed in ref 42. These corrections are needed to obtain reliable optical constants for powdered samples. The agreement of the phonon lifetimes, Born charges, and force constants for single crystalline and bulk powdered 2H-MoS_2 demonstrate the viability of this approach.

Figure 2a displays a close-up view of the infrared reflectance spectra of 2H-, IF-, and Re(0.18%):IF-MoS_2 at 300 K. Two vibrational modes are observed, which is in agreement with group theory predictions for the 2H- polytype.[35−38] We assign the 384 cm^{-1} peak to the E_{1u} mode and the 468 cm^{-1} structure to the A_{2u} mode. These spectral features probe intralayer and interlayer dynamics, respectively (insets, Figure 1). The overall

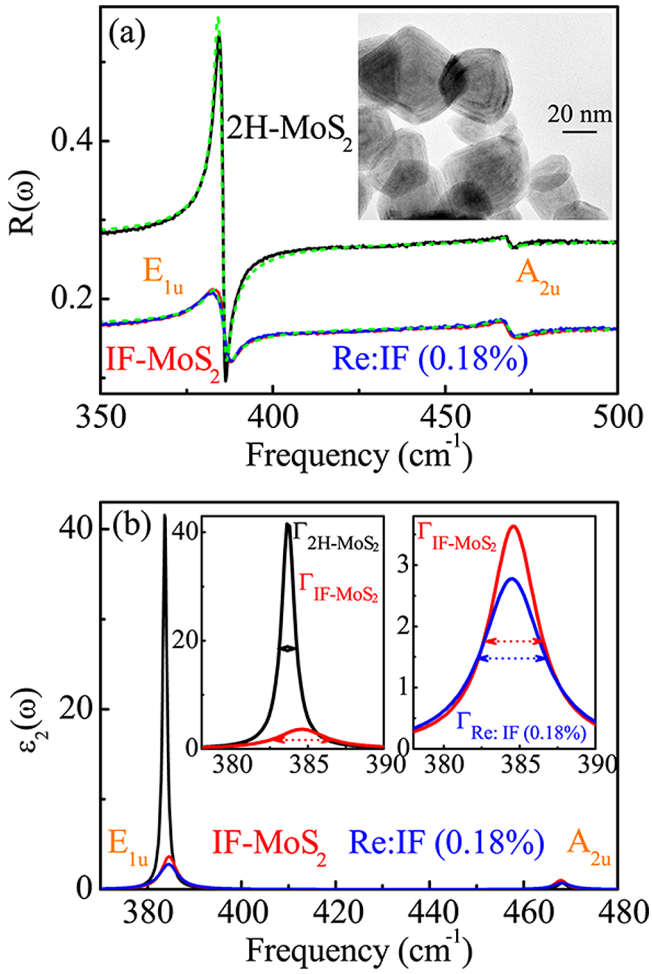

Figure 2. (a) Close-up view of the infrared reflectance of 2H-, IF-, and Re:IF-(0.18%) MoS_2, corrected for scattering effects,[42,44] at 300 K. Black, red, and blue curves correspond to the 2H-, IF-, and Re-substituted materials respectively. Green dashed lines show the theoretical fit as described in the text. Inset: high resolution transmission electron microscopy image of the IF-MoS_2 nanoparticles. (b) $\varepsilon_2(\omega)$ of 2H, IF-, Re:IF-MoS_2 calculated from an oscillator fit of the reflectance. Left inset: close-up view of $\varepsilon_2(\omega)$ comparing 2H- and IF-MoS_2 in the vicinity of the E_{1u} mode. Right inset: $\varepsilon_2(\omega)$ for IF- and Re:IF-MoS_2.

number and position of the phonons is in good agreement with previous single crystal data[41] and represents the main evidence for local 2H- character in the nanoparticles. Striking linewidth and intensity changes are also immediately apparent in the data, especially when comparing the 2H- and pristine IF-response.[41,42] E_{1u} and A_{2u} mode character also change with doping, although the differences are more subtle. We quantified these effects using classical dielectric oscillator models[41,43] and appropriate density, orientation, and scattering corrections.[42,44] The parameters extracted from this analysis are summarized in Table 1 and Supporting Information Table S1 and are employed to understand phonon lifetimes and chemical bonding in these nanoscale chalcogenides.

Figure 2b displays the dielectric response $\varepsilon_2(\omega)$ of 2H-, IF-, and Re(0.18%):IF-MoS_2. Inspection immediately reveals that damping is significantly larger in the nanoparticles than in the bulk. We can understand this effect and the doping-induced trends in terms of phonon lifetimes. Here's how they are related. The full width at half-maximum can be estimated

dx.doi.org/10.1021/nl401066e | Nano Lett. 2013, 13, 2803−2808

Table 1. Intrinsic Oscillator Parameters and Lifetimes of 2H-, IF-, and Re:IF-MoS_2[a]

material	mode	$\omega_{TO,j}$ (cm^{-1})	γ	τ (ps)
2H-MoS_2	E_{1u}	384[b]	0.0025[b]	5.5
single crystal[b]	A_{2u}	470[b]	0.005[b]	2.3
2H-MoS_2	E_{1u}	383.7	0.0027	5.1
powder	A_{2u}	468.2	0.0053	2.1
IF-MoS_2	E_{1u}	384.6	0.0099	1.4
	A_{2u}	467.9	0.0067	1.7
Re:IF-MoS_2	E_{1u}	384.4	0.0105	1.3
(0.0106%)	A_{2u}	468.5	0.0077	1.5
Re:IF-MoS_2	E_{1u}	384.5	0.0125	1.1
(0.18%)	A_{2u}	468.2	0.0098	1.2

[a]Intrinsic oscillator parameters of 2H-, IF-, and Re:IF-MoS_2 extracted from an oscillator fit of the reflectance and after scattering, orientational, and density corrections.[42,44] Some segregation of ReS_2 islands may occur, especially at the highest doping levels.[19] Error bars are ± 1 cm^{-1} for $\omega_{TO,E_{1u}}$, ± 1 cm^{-1} for $\omega_{TO,A_{2u}}$, ± 0.0005 for $\gamma_{E_{1u}}$, ± 0.0007 for $\gamma_{A_{2u}}$, ± 0.1 ps for $\tau_{E_{1u}}$, and ± 0.2 ps for $\tau_{A_{2u}}$. [b]Single crystal data from ref 41.

directly from the spectral data as $\Gamma = \gamma\omega_{TO}$, where γ is the damping constant and ω_{TO} is the transverse phonon frequency. These Γ's can be converted to effective phonon lifetimes as $\tau = \hbar/\Gamma$, where, $\hbar$ is the reduced Planck constant ($\hbar = h/2\pi$).[45] Analysis of the spectral data of Wieting and Verble[41] reveals effective phonon lifetimes of 5.5 and 2.3 ps for the E_{1u} and A_{2u} modes of single crystalline 2H-MoS_2. These values compare reasonably with the τ's of other traditional semiconductors. For instance, τ is 5 ps in GaAs and 10 ps in GaN.[4,8] Moreover, the agreement between single crystal and bulk powder lifetimes in MoS_2 indicates that our technique[42,44] accounts for the nature of powdered materials reasonably well.

The effective phonon lifetime decreases from 5.5 ps in the single crystal to 1.4 ps in the nanoparticles. Clearly, size has a major effect on τ.[12,42] Employing a characteristic phonon velocity of 300 m/s, we find mean free paths of 1.75 and 0.28 nm in 2H- and IF-MoS_2, respectively. These length scales are equivalent to a single MoS_2 fragment. By comparison, the lifetime of the G-mode in single wall carbon nanotubes is 1.1 ps.[5] Doping in IF-MoS_2 also reduces τ, but the effect is more modest.[46] Table 1 summarizes our findings.

Phonon lifetimes can be determined and their trends understood by accounting for different scattering contributions according to Matthiessen's rule[47−49]

$$\frac{1}{\tau} = \frac{1}{\tau_u} + \frac{1}{\tau_b} + \frac{1}{\tau_m} + \frac{1}{\tau_{e-ph}} \quad (1)$$

This expression allows consideration of microscopic effects including three-phonon Umklapp, boundary, mass-difference, and electron−phonon scattering. These effects are diagrammed in Figure 3. The overall phonon lifetime is determined by summing inverse lifetimes for each mechanism. Naturally, different terms dominate depending upon the situation. For instance, $1/\tau_u$, is proportional to temperature, and because our measurements are conducted at 300 K, we can neglect Umklapp effects in our analysis. The other scattering mechanisms in eq 1 contribute to size and doping effects as discussed below.

Let us begin by considering size effects. Table 1 reveals that τ for the E_{1u} mode decreases from 5.5 ps in the 2H-MoS_2 single crystal to 1.4 ps in IF-MoS_2. The contribution of τ_b to the total phonon lifetime captures the size effect (eq 1). Boundary scattering effects can be expressed as $(1/\tau_b) \propto (1 - p)$, where p is the boundary parameter, and $p = 1$ is the limiting case of purely specular scattering.[48,49] This model implies that smaller particles should have shorter lifetime. We therefore attribute the dramatically decreased phonon lifetime in the 50−140 nm diameter IF-MoS_2 nanoparticles to boundary scattering effects.[12,50] Another interesting result pertains to the A_{2u} mode behavior. Examination of Table 1 shows that the phonon lifetime is reduced from 2.3 ps in the single crystal to 1.7 ps in IF-MoS_2, which is a much smaller change that that observed for

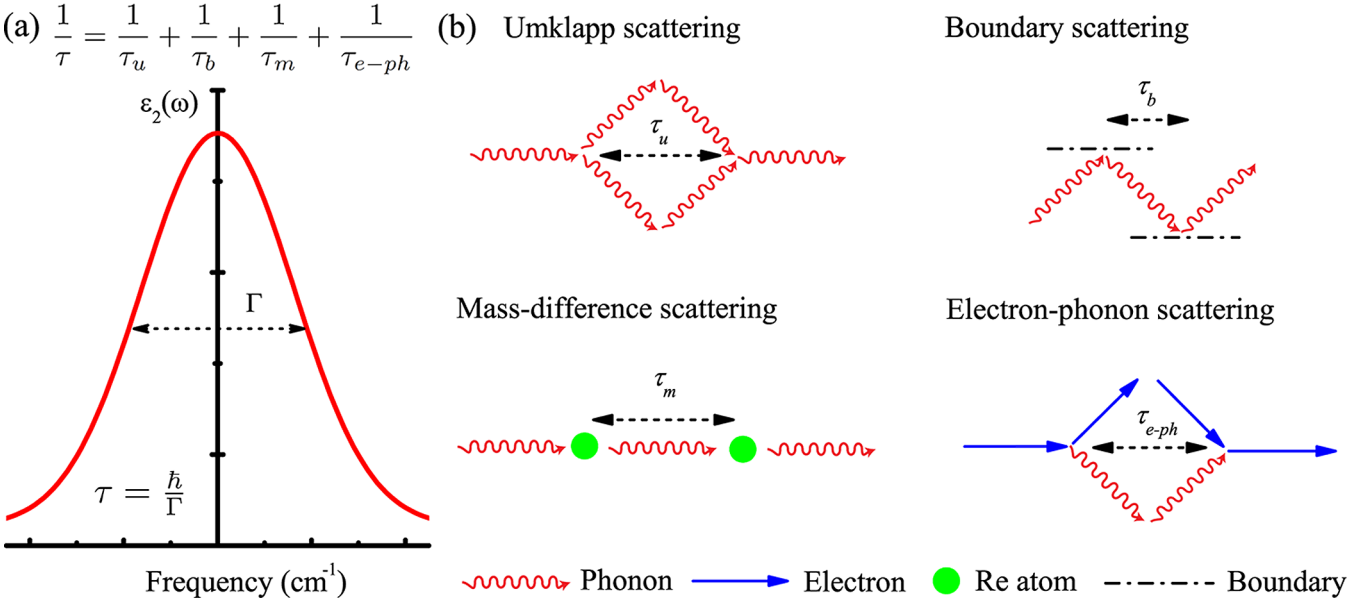

Figure 3. (a) Schematic approach to the experimental determination of phonon lifetimes. The upper equation includes several possible contributions to the overall phonon lifetime, τ, based upon Matthiessen's rule.[47,48] (b) Schematic views of three-phonon Umklapp scattering, boundary scattering, mass-difference scattering, and electron−phonon scattering mechanisms.[49].

dx.doi.org/10.1021/nl401066e | Nano Lett. 2013, 13, 2803−2808

the E_{1u} mode. This effect may be due to the weak van der Waals interactions between layers and smaller structural strains.[42]

Doping is different. From Table 1, we see that τ for the E_{1u} mode decreases from 1.4 ps in IF-MoS_2 to 1.1 ps in the most heavily substituted sample. We attribute these small but systematic trends in the overall phonon lifetime to a combination of two effects: mass-difference scattering, τ_m, and phonon−electron scattering, τ_{e-ph}.[49] In the first case, $(1/\tau_m) \propto \sum f_{Re}(1 - (m_{Re}/\bar{m}))^2$, where f_{Re} is the fractional concentration of Re centers, m_{Re} is the mass of Re atom, and $\bar{m} = f_{Re}m_{Re} + f_{Mo}m_{Mo}$ is the average atomic mass.[48,49] As doping increases, the lifetime becomes shorter. The electron−phonon scattering contribution can be expressed as $(1/\tau_{e-ph}) \propto n$, where n is carrier density.[48,49] We already know from our prior work that the relationship between actual doping level and carrier density is described by the Burstein−Moss shift.[27] Thus the portion of the overall lifetime due to electron−phonon scattering effects is anticipated to decrease at higher Re concentrations. Another interesting result pertains to the behavior of the A_{2u} mode. Doping-induced changes in τ are actually larger than for the E_{1u} mode, a finding that we attribute to intra- versus interlayer dc conductivity differences[51] rather than structural effects.

It is well-known that carrier mobilities and dynamical processes in polar semiconductors such as GaAs are determined by the interaction between carriers and optical phonons.[11] Short phonon lifetimes imply stronger carrier-phonon interactions whereas long lifetimes indicate fewer scattering events in the system.[48,49] Re doping of IF-MoS_2 decreases τ, so this system falls into the category for which carrier−phonon scattering is of greater importance. Essentially, doping (or applied electric field) offers a trade-off: control of carrier density versus increased scattering. These considerations impact a number of engineering properties. For instance, optical phonon lifetimes are also useful in determining the total energy loss rate of the carriers.[10,52] When the characteristic size of various electronics components is reduced into the nanoscale size regime, quantum confinement can modify the hot-electron energy relaxation rate compared with the bulk-phonon emission case.[10] This is important for semiconductor quantum-well lasers because it determines the minimum time needed for on−off switching.[10] Charge recombination limits solar cell and photocatalytic efficiencies as well.[53,54] Adding carriers via chemical doping also increases interparticle electrostatic repulsion, which improves rheological and tribological behavior.[30]

Vibrational spectroscopy also supports an analysis of chemical bonding. In prior work, we demonstrated that small size reduces the Born effective charge of IF-MoS_2 compared to that in the 2H- material,[42] a development attributed to strain and curvature in the nanoparticles. This physical effect manifests itself as a reduction of polarizability in the interlayer direction (Table 2). The reduced polarizability[42] of the nanoparticles compared to the single crystal indicates improved electron cloud overlap (which favors stronger covalent interactions).[55] While covalent interactions increase with decreasing size, ionicity (as quantified by the local charge Z^*) remains the same. This overall stronger chemical bonding may contribute to the reduced friction coefficient at high loads in the nanolubricant.[20,56] The availability of Re-substitited nanoparticles allows us to extend this analysis. We find essentially no change in the Born charges of Re:IF-MoS_2 compared to IF-MoS_2 at any doping level studied here (Table 2). The extra carriers from the doping process should therefore be considered as only small perturbations on heavy ions.[57] Similar local effective charges imply that ionic interactions are independent of doping. The force constants[42] are insensitive to both size and chemical doping as well, a finding that reinforces our conclusion that ionicity does not drive the novel properties.

Table 2. Born Effective Charges (Z^*_B), Polarizability (α), Local Effective Charge (Z^*), and the Force Constant (k) of 2H-, IF-, and Re:IF-MoS_2 in the Two Principle Directions[a]

material	mode	Z^*_B (e)	α (Å^3)	Z^* (e)	k (N/m)
2H-MoS_2	E_{1u}	1.11	100	0.15	336
single crystal	A_{2u}	0.52	200	0.37	501
2H-MoS_2	E_{1u}	1.11	100	0.15	336
powder	A_{2u}	0.52	200	0.37	497
IF-MoS_2	E_{1u}	0.69	91	0.16	338
	A_{2u}	0.52	200	0.37	497
Re:IF-MoS_2	E_{1u}	0.69	91	0.16	337
(0.0106%)	A_{2u}	0.52	200	0.37	498
Re:IF-MoS_2	E_{1u}	0.68	91	0.16	338
(0.18%)	A_{2u}	0.52	200	0.37	497

[a]Because Born charge contains both dynamic and static contributions, we decompose it into total polarizability (α) and local effective charge (Z^*). Here α is the sum of cationic and anionic electron cloud volume contributions, whereas local effective charge indicates the ionicity of a material.[42,44]

To summarize, we investigated the infrared vibrational properties of pristine and Re-substituted MoS_2 nanoparticles, extracted phonon lifetimes, and analyzed the τ's in terms of multiple scattering events. Our measurements reveal that while the lifetime of 2H-MoS_2 is similar to that of traditional polar semiconductors like GaAs, τ of the nanoparticles is 50% smaller due to grain boundary scattering. The n-doping reduces the lifetime even further, a trend that we attribute to combined charge and mass effects. These findings are important for understanding carrier−phonon interactions in low-dimensional semiconducting nanomaterials. They also illustrate the utility of reaching beyond conventional bulk semiconductors and quantum dots to explore how doping and confinement underpin performance metrics like mobility and carrier dynamics in layered systems.

■ ASSOCIATED CONTENT

Supporting Information

A spectroscopic analysis of local structure and symmetry along with a detailed discussion of the charge and bonding analysis. This material is available free of charge via the Internet at http://pubs.acs.org.

■ AUTHOR INFORMATION

Corresponding Author

*E-mail: musfeldt@utk.edu.

Present Address

§(Q.-C.S.) Department of Chemical and Biological Engineering, University of Colorado, Boulder, Colorado 80309 United States.

Notes

The authors declare no competing financial interest.

■ ACKNOWLEDGMENTS

This research is supported by the U.S. Department of Energy, Office of Basic Energy Sciences, Division of Materials Sciences

and Engineering under Award DE-FG02-01ER45885 (J.L.M.) and NanoMaterials, Ltd. (Weizmann). R.T. is the director of the Helen and Martin Kimmel Center for Nanoscale Science and holds the Drake Family Chair in Nanotechnology.

REFERENCES

(1) Sootsman, J. R.; Chung, D. Y.; Kanatzidis, M. G. New and Old Concepts in Thermoelectric Materials. *Angew. Chem., Int. Ed.* **2009**, *48*, 8616−8639.

(2) Cheong, S. W.; Mostovoy, M. Multiferroics: a Magnetic Twist for Ferroelectricity. *Nat. Mater.* **2007**, *6*, 13−20.

(3) Dresselhaus, M. S.; Chen, G.; Tang, M. Y.; Yang, R. G.; Lee, H.; Wang, D. Z.; Ren, Z. F.; Fleurial, J. P.; Gogna, P. New Directions for Low-Dimensional Thermoelectric Materials. *Adv. Mater.* **2007**, *19*, 1043−1053.

(4) Bergman, L.; Alexson, D.; Murphy, P. L.; Nemanich, R. J.; Dutta, M.; Stroscio, M. A.; Balkas, C.; Shin, H.; Davis, R. F. Raman Analysis of Phonon Lifetimes in AlN and GaN of Wurtzite Structure. *Phys. Rev. B* **1999**, *59*, 12977−12982.

(5) Song, D.; Wang, F.; Dukovic, G.; Zheng, M.; Semke, E. D.; Brus, L. E.; Heinz, T. F. Direct Measurement of the Lifetime of Optical Phonons in Single-Walled Carbon Nanotubes. *Phys. Rev. Lett.* **2008**, *100*, 225503.

(6) Debernardi, A. Phonon Linewidth in III-V Semiconductors From Density-Functional Perturbation Theory. *Phys. Rev. B* **1998**, *57*, 12847−12858.

(7) Vonderlinde, D.; Kuhl, J.; Klingenberg, H. Raman Scattering from Nonequilibrium LO Phonons with Picosecond Resolution. *Phys. Rev. Lett.* **1980**, *44*, 1505−1508.

(8) Shah, J.; Leite, R. C. C.; Scott, J. F. Photoexcited Hot LO Phonons in GaAs. *Solid State Commun.* **1970**, *8*, 1089−1093.

(9) Menendez, J.; Cardona, M. Temperature Dependence of the First-Order Raman Scattering by Phonons in Si, Ge, and α-Sn: Anharmonic Effects. *Phys. Rev. B* **1984**, *29*, 2051−2059.

(10) Campos, V. B.; Dassarma, S.; Stroscio, M. A. Phonon Confinement Effect on Electron Energy Loss in One-Dimensional Quantum Wires. *Phys. Rev. B* **1992**, *46*, 3849−3853.

(11) Bhatt, A. R.; Kim, K. W.; Stroscio, M. A. Theoretical Calculation of Longitudinal-Optical-Phonon Lifetime in GaAs. *J. Appl. Phys.* **1994**, *76*, 3905−3907.

(12) Fu, X. G.; An, H. Z.; Du, W. M. Temperature-Dependent Raman Scattering Studies in ZnSe Nanoparticles. *Mater. Lett.* **2005**, *59*, 1484−1490.

(13) Kumar, C. S. S. R. *Raman Spectroscopy for Nanomaterials Characterization*; Springer: New York, 2012.

(14) Tenne, R. Inorganic Nanotubes and Fullerene-Like Nanoparticles. *Nat. Nanotechnol.* **2006**, *1*, 103−111.

(15) Castellanos-Gomez, A.; Poot, M.; Steele, G. A.; van der Zant, H. S. J.; Agrait, N.; Rubio-Bollinger, G. Elastic Properties of Freely Suspended MoS_2 Nanosheets. *Adv. Mater.* **2012**, *24*, 772−775.

(16) Kou, L.; Tang, C.; Zhang, Y.; Heine, T.; Chen, C.; Frauenheim, T. Tuning Magnetism and Electronic Phase Transitions by Strain and Electric Field in Zigzag MoS_2 Nanoribbons. *J. Phys. Chem. Lett.* **2012**, *3*, 2934−2941.

(17) Deepak, F. L.; Popovitz-Biro, R.; Feldman, Y.; Cohen, H.; Enyashin, A.; Seifert, G.; Tenne, R. Fullerene-Like $Mo(W)_{1-x}Re_xS_2$ Nanoparticles. *Chem. Asian J.* **2008**, *3*, 1568−1574.

(18) Rosentsveig, R.; Margolin, A.; Gorodnev, A.; Popovitz-Biro, R.; Feldman, Y.; Rapoport, L.; Novema, Y.; Naveh, G.; Tenne, R. Synthesis of Fullerene-Like MoS_2 Nanoparticles and Their Tribological Behavior. *J. Mater. Chem.* **2009**, *19*, 4368−4374.

(19) Yadgarov, L.; Stroppa, D. G.; Rosentsveig, R.; Ron, R.; Enyashin, A. N.; Houben, L.; Tenne, R. Investigation of Rhenium Doped MoS_2 Nanoparticles with Fullerene-Like Structure (IF-MoS_2). *Z. Anorg. Allg. Chem.* **2012**, *638*, 2610−2616.

(20) Yadgarov, L.; Rosentsveig, R.; Leitus, G.; Albu-Yaron, A.; Moshkovich, A.; Perfilyev, V.; Vasic, R.; Frenkel, A. I.; Enyashin, A. N.; Seifert, G. Controlled Doping of MS_2 (M = W, Mo) Nanotubes and Fullerene-Like Nanoparticles. *Angew. Chem., Int. Ed.* **2012**, *51*, 1148−1151.

(21) Seifert, G.; Terrones, H.; Terrones, M.; Jungnickel, G.; Frauenheim, T. Structure and Electronic Properties of MoS_2 Nanotubes. *Phys. Rev. Lett.* **2000**, *85*, 146−149.

(22) Popov, I.; Pecchia, A.; Okano, S.; Ranjan, N.; Di Carlo, A.; Seifert, G. Electronic and Transport Properties of Contacts Between Molybdenum Sulfide Nanowires and Gold Electrodes. *Appl. Phys. Lett.* **2008**, *93*, 083115.

(23) Radisavljevic, B.; Radenovic, A.; Brivio, J.; Giacometti, V.; Kis, A. Single-Layer MoS_2 Transistors. *Nat. Nanotechnol.* **2011**, *6*, 147−150.

(24) Ramasubramaniam, A.; Naveh, D.; Towe, E. Tunable Band Gaps in Bilayer Transition-Metal Dichalcogenides. *Phys. Rev. B* **2011**, *84*, 205325.

(25) Ye, J. T.; Zhang, Y. J.; Akashi, R.; Bahramy, M. S.; Arita, R.; Iwasa, Y. Superconducting Dome in a Gate-Tuned Band Insulator. *Science* **2012**, *388*, 1193−1196.

(26) Wang, Q. H.; Kalantar-Zadeh, K.; Kis, A.; Coleman, J. N.; Strano, M. S. Electronics and Optoelectronics of Two-Dimensional Transition Metal Dichalcogenides. *Nat. Nanotechnol.* **2012**, *7*, 699−712.

(27) Sun, Q. -C.; Yadgarov, L.; Rosentsveig, R.; Seifert, G.; Tenne, R.; Musfeldt, J. L. Observation of a Burstein-Moss Shift in Re-Doped MoS_2 Nanoparticles. *ACS Nano* **2013**, *7*, 3506−3511.

(28) Enyashin, A. N.; Yadgarov, L.; Houben, L.; Popov, I.; Weidenbach, M.; Tenne, R.; Bar-Sadan, M.; Seifert, G. New Route for Stabilization of 1T-WS_2 and MoS_2 Phases. *J. Phys. Chem. C* **2011**, *115*, 24586−24591.

(29) Tevet, O.; Von-Huth, P.; Popovitz-Biro, R.; Rosentsveig, R.; Wagner, H. D.; Tenne, R. Friction Mechanism of Individual Multilayered Nanoparticles. *Proc. Natl. Acad. Sci. U.S.A.* **2011**, *108*, 19901−19906.

(30) Rapoport, L.; Moshkovich, A.; Perfilyev, V.; Laikhtman, A.; Lapsker, I.; Yadgarov, L.; Rosentsveig, R.; Tenne, R. High Lubricity of Re-Doped Fullerene-Like MoS_2 Nanoparticles. *Tribol. Lett.* **2012**, *45*, 257−264.

(31) Yadgarov, L.; Petrone, V.; Rosentsveig, R.; Feldman, Y.; Tenne, R.; Senatore, A. Tribological Studies of Rhenium Doped Fullerene-Like MoS_2 Nanoparticles in Boundary, Mixed and Elasto-Hydrodynamic Lubrication Conditions. *Wear* **2013**, *297*, 1103−1110.

(32) Mocatta, D.; Cohen, G.; Schattner, J.; Millo, O.; Rabani, E.; Banin, U. Heavily Doped Semiconductor Nanocrystal Quantum Dots. *Science* **2011**, *332*, 77−81.

(33) Amasha, S.; Keller, A. J.; Rau, I. G.; Carmi, A.; Katine, J. A.; Shtrikman, H.; Oreg, Y.; Goldhaber-Gordon, D. Pseudospin-Resolved Transport Spectroscopy of the Kondo Effect in a Double Quantum Dot. *Phys. Rev. Lett.* **2013**, *110*, 046604.

(34) Zak, A.; Feldman, Y.; Alperovich, V.; Rosentsveig, R.; Tenne, R. Growth Mechanism of MoS_2 Fullerene-Like Nanoparticles by Gas-Phase Synthesis. *J. Am. Chem. Soc.* **2000**, *122*, 11108−11116.

(35) The structure of 2H-MoS_2 belongs to the $P6_3/mmc$ space group.[36] The atomic centers (six per primitive cell) are arranged in sheets parallel to the base of the hexagonal unit cell. Each MoS_2 slab contains a layer of metal centers, sandwiched between two chalcogen layers, with each metal atom bonded to six chalcogen atoms in a trigonal prismatic arrangement (D_{3h} local symmetry). Group theory predicts two infrared active E_{1u} and A_{2u} modes.[37,38] These modes are sensitive to phonon lifetimes and chemical bonding in the intralayer and interlayer directions.

(36) Schonfeld, B.; Huang, J. J.; Moss, S. C. Anisotropic Mean-Square Displacements (MSD) in Single-Crystals of 2H- and 3R-MoS_2. *Acta Cryst. B* **1983**, *39*, 404−407.

(37) Verble, J. L.; Wieting, T. J. Lattice Mode Degeneracy in MoS_2 and Other Layer Compounds. *Phys. Rev. Lett.* **1970**, *25*, 362−365.

(38) Luttrell, R. D.; Brown, S.; Cao, J.; Musfeldt, J. L.; Rosentsveig, R.; Tenne, R. Dynamics of Bulk Versus Nanoscale WS_2: Local Strain and Charging Effects. *Phys. Rev. B* **2006**, *73*, 035410.

(39) Pellets were prepared with very modest pressure, so we do not anticipate that density will approach that of a single crystal as it would if high pressures were employed.
(40) We select this approach rather than a Kramers–Kronig analysis to better connect with prior work on 2H-MoS_2 single crystals.[41,43] The Kramers–Kronig approach[45] yields the same conclusions.
(41) Wieting, T. J.; Verble, J. L. Infrared and Raman Studies of Long-Wavelength Optical Phonons in Hexagonal MoS_2. *Phys. Rev. B* **1971**, *3*, 4286–4292.
(42) Sun, Q. C.; Xu, X. S.; Vergara, L. I.; Rosentsveig, R.; Musfeldt, J. L. Dynamical Charge and Structural Strain in Inorganic Fullerenelike MoS_2 Nanoparticles. *Phys. Rev. B* **2009**, *79*, 205405.
(43) Lucovsky, G.; White, R. M.; Benda, J. A.; Revelli, J. F. Infrared-Reflectance Spectra of Layered Group-IV and Group-VI Transition-Metal Dichalcogenides. *Phys. Rev. B* **1973**, *7*, 3859–3870.
(44) Sun, Q. C.; Xu, X. S.; Baker, S. N.; Christianson, A. D.; Musfeldt, J. L. Experimental Determination of Ionicity in MnO Nanoparticles. *Chem. Mater.* **2011**, *23*, 2956–2960.
(45) Wooten, F. *Optical Properties of Solids*; Academic Press: New York, 1972.
(46) Beechem, T.; Graham, S. Temperature and Doping Dependence of Phonon Lifetimes and Decay Pathways in GaN. *J. Appl. Phys.* **2008**, *103*, 093507.
(47) Matthiessen, A.; Vogt, C. On the Influence of Temperature on the Electric Conducting-Power of Alloys. *Philos. Trans. R. Soc. London* **1864**, *154*, 167–200.
(48) Kittel, C. *Introduction to Solid State Physics*; Wiley: New York, 2004.
(49) Zou, J.; Balandin, A. Phonon Heat Conduction in a Semiconductor Nanowire. *J. Appl. Phys.* **2001**, *89*, 2932–2938.
(50) The modest difference between the single crystal and bulk powder τ's in Table 1 is also related to boundary scattering from the ~44 μm average particulate size of the powder sample.
(51) El-Mahalawy, S. H.; Evans, B. L. Temperature Dependence of the Electrical Conductivity and Hall Coefficient in 2H-MoS_2, $MoSe_2$, WSe_2, and $MoTe_2$. *Phys. Status Solidi B* **1977**, *79*, 713–722.
(52) Wang, K.; Simon, J.; Goel, N.; Jena, D. Optical study of Hot Electron Transport in GaN: Signatures of the Hot-Phonon Effect. *Appl. Phys. Lett.* **2006**, *88*, 022103.
(53) Shanmugam, M.; Bansal, T.; Durcan, C. A.; Yu, B. Molybdenum Disulphide/Titanium Dioxide Nanocomposite-Poly 3-Hexylthiophene Bulk Heterojunction Solar Cell. *Appl. Phys. Lett.* **2012**, *100*, 153901.
(54) Subramanian, V.; Wolf, E. E.; Kamat, P. V. Green Emission to Probe Photoinduced Charging Events in ZnO-Au Nanoparticles. Charge Distribution and Fermi-Level Equilibration. *J. Phys. Chem. B* **2003**, *107*, 7479–7485.
(55) Masenelli, B.; Nicolas, D.; Melinon, P. Is a Highly Ionic Material Still Ionic as a Nanoparticle? *Small* **2008**, *4*, 1233–1239.
(56) Stefanov, M.; Enyashin, A. N.; Heine, T.; Seifert, G. Nanolubrication: How Do MoS_2-Based Nanostructures Lubricate? *J. Phys. Chem. C.* **2008**, *112*, 17764–17767.
(57) Frey, G. L.; Elani, S.; Homyonfer, M.; Feldman, Y.; Tenne, R. Optical-Absorption Spectra of Inorganic Fullerenelike MS_2 (M = Mo, W). *Phys. Rev. B* **1998**, *57*, 6666–6671.